AGU PUBLICATIONS

Geophysical Research Letters

RESEARCH LETTER
10.1002/2017GL072964

Key Points:
- Submarine braided channels on a submarine fan exhibit active channels and nonactive channels
- Active and total braiding intensities of experimental submarine braided channels are proportional to discharge and slope at steady state
- Active braiding intensity of experimental submarine braided channels scales linearly with dimensionless stream power

Supporting Information:
- Supporting Information S1
- Movie S1
- Movie S2

Correspondence to:
S. Y. J. Lai
stevenyjlai@mail.ncku.edu.tw

Citation:
Lai, S. Y. J., S. S. C. Hung, B. Z. Foreman, A. B. Limaye, J.-L. Grimaud, and C. Paola (2017), Stream power controls the braiding intensity of submarine channels similarly to rivers, *Geophys. Res. Lett.*, *44*, doi:10.1002/2017GL072964.

Received 5 FEB 2017
Accepted 8 MAY 2017
Accepted article online 10 MAY 2017

Stream power controls the braiding intensity of submarine channels similarly to rivers

Steven Y. J. Lai[1], Samuel S. C. Hung[1], Brady Z. Foreman[2], Ajay B. Limaye[3], Jean-Louis Grimaud[4], and Chris Paola[3]

[1]Department of Hydraulic and Ocean Engineering, National Cheng Kung University, Tainan, Taiwan, [2]Department of Geology, Western Washington University, Bellingham, Washington, USA, [3]Department of Earth Sciences, St. Anthony Falls Laboratory, University of Minnesota, Twin Cities, Minneapolis, Minnesota, USA, [4]MINES ParisTech, Centre de Géosciences, PSL Research University, Fontainebleau, France

Abstract We use physical experiments to investigate the response of submarine braided channels driven by saline density currents to increasing inflow discharge and bed slope. We find that, similarly to braided rivers, only a fraction of submarine braided networks have active sediment transport. We then find similar response to imposed change between submarine and fluvial braided systems: (1) both the active and total braiding intensities increase with increasing discharge and slope; (2) the ratio of active braiding intensity to total braiding intensity is 0.5 in submarine braided systems regardless of discharge and slope; and (3) the active braiding intensity scales linearly with dimensionless stream power. Thus, braided submarine channels and braided rivers are similar in some important aspects of their behavior and responses to changes in stream power and bed slope. In light of the scale independence of braided channel planform organization, these results are likely to apply beyond experimental scales.

1. Introduction

Submarine channels have long been recognized in canyons, on fans, and across deep-sea plains and represent major conduits for sediment routing along continental margins. The planform geometry, deposits, and flow patterns of deep water sinuous channels have been examined using methods including sonar and in situ measurements [*Deptuck et al.*, 2007; *Kertznus and Kneller*, 2009; *Amblas et al.*, 2012; *Wynn et al.*, 2014]. These studies identified distinctive features of submarine channels relative to rivers, including reversed helical flow patterns, ossification of channel mobility, comparable in-channel and overbank sedimentation rates, and the potential influence of Coriolis forces on channel sinuosity [*Peakall et al.*, 2000; *Wynn et al.*, 2007; *Flood et al.*, 2009; *Babonneau et al.*, 2010; *Parsons et al.*, 2010; *Kolla et al.*, 2012; *Peakall et al.*, 2012; *Sumner et al.*, 2014].

The work above has focused on submarine single-thread sinuous channels; relatively, little research addresses the existence of submarine braided channels and their potential similarities or dissimilarities with braided fluvial systems. The rarity of braided submarine channels seems to suggest that the conditions under which rivers form multiple braided channels [*Parker*, 1976; *Ashmore*, 1982, 1991; *Tal and Paola*, 2007] are not as easily achieved by submarine density (turbidity) currents. It is still unclear whether submarine braided channels behave similarly to braided rivers, which often occur on steep slopes and have small channel (aspect) depth-width ratios, consistent with theoretical predictions [*Parker*, 1976]. Recent work shows that submarine braiding occurs at channel aspect ratios similar to braided rivers [*Foreman et al.*, 2015]. However, fundamental questions about channel pattern dynamics and their response to changing flow discharge and slope still remain to be addressed. The combination of discharge and slope strongly influences braided channel geometry, planform morphology, spatial distribution of sediment transport, channel aspect ratio, and hence pattern dynamics [*Parker*, 1976; *Parker et al.*, 2007; *Egozi and Ashmore*, 2008, 2009; *Kleinhans et al.*, 2014]. Do submarine braided channels behave similarly? In this study, we investigate how total braiding intensity (BI_T) and active braiding intensity (BI_A)—defined as the total number and number of actively transporting channels [*Egozi and Ashmore*, 2008, 2009]—respond to changes in slope and discharge in submarine braided channels. We find that the response generally parallels that in braided rivers.

2. Experimental Design and Procedure

Physical experiments are commonly employed to examine the evolution of sedimentary systems in response to known forcing mechanisms, and the strengths and limitations of experiments have been extensively

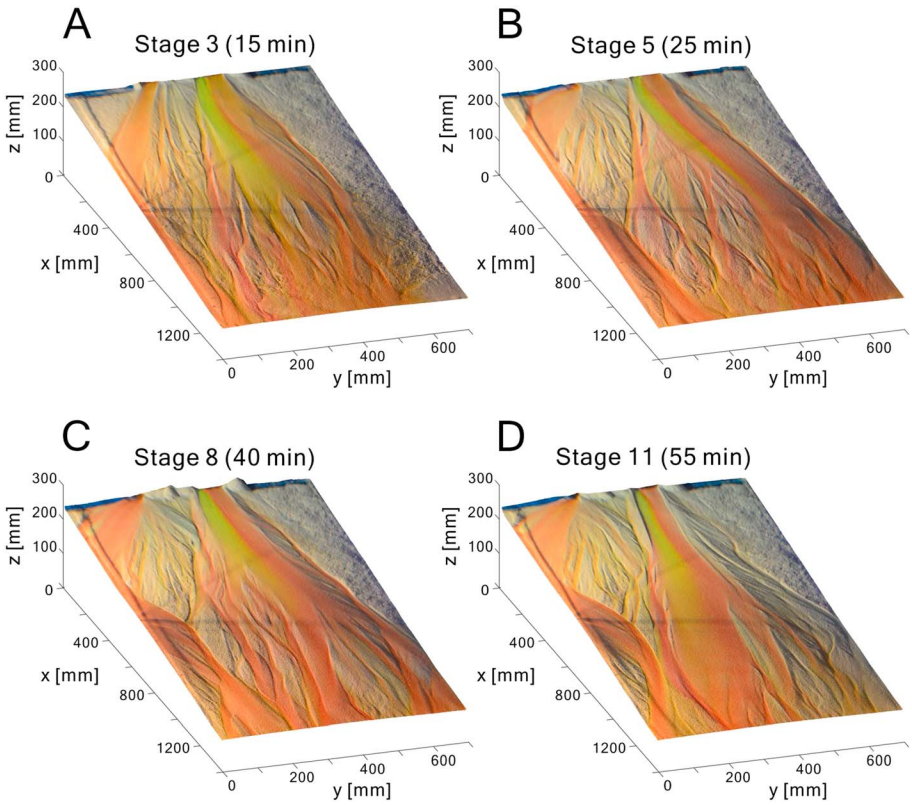

Figure 1. Digital elevation models (DEMs) with draped color orthophotos of Stages 3, 5, 8, and 11 (time = 15, 25, 40, and 55 min, respectively) of Run A3. Unconfined fluorescent saline underflows (in green and red) move from the top to the bottom of each DEM. Movie S1 in the supporting information shows channel dynamics that occur throughout the experiment.

discussed [*Malverti et al.*, 2008; *Paola et al.*, 2009; *Lajeunesse et al.*, 2010; *Kleinhans et al.*, 2014]. Physical experiments have been especially useful in studying turbidity currents, which in nature are rare, difficult to predict, occur underwater, and commonly at great depth, and can damage or destroy measurement instruments. Recent experimental studies of submarine channels have addressed submarine channel initiation and development [*Métivier et al.*, 2005; *Yu et al.*, 2006; *Cantelli et al.*, 2011], submarine canyon evolution [*Weill et al.*, 2014; *Lai et al.*, 2016], and flow and sedimentation patterns in prescribed submarine sinuous channels [*Peakall et al.*, 2007; *Straub et al.*, 2008]. With few exceptions [*Rowland et al.*, 2010; *Foreman et al.*, 2015], previous studies focus on sinuous and/or erosional channels.

We conducted experiments in a shallow sedimentary basin (1.40 m long × 0.70 m wide × 0.06 m deep) submerged in a water tank (1.50 m long × 0.90 m wide × 0.60 m deep) (supporting information Figure S1). The bed comprises plastic sediment (d_{50} = 0.34 mm, specific gravity = 1.5) 0.04 m deep, with variable slope. Upstream, a tunnel and three equally spaced reservoirs (0.1 m long × 0.1 m wide × 0.04 m deep) were placed ahead of the submerged basin for mixing inflow and sediment. We released a steady saline inflow (specific gravity = 1.2, dyed fluorescent green), as a proxy for mud-rich turbidity currents [*Métivier et al.*, 2005; *Lai and Capart*, 2007, 2009; *Weill et al.*, 2014; *Foreman et al.*, 2015; *Lai et al.*, 2016]. Along with the flow, we introduced dry plastic sediment equivalent to the bed material to simulate continuous sediment gravity flows transporting sediment in traction across the seabed. We present six experimental runs (grouped into Series A and B) with increasing inflow discharge and basement slope, respectively (see Table S1 for the controlled parameters). Each run was divided into 15 to 20 successive stages, each of 5 min duration. During the experiment, we took oblique-view photographs from outside the water basin every 5 s to record channel evolution. We injected red dye from the middle upstream source during the last 60 s of each stage to distinguish the instantaneous flow pattern (red) from the continuous (green) flow and highlight the depositional bar structure. At the end of each stage, without draining the ambient water,

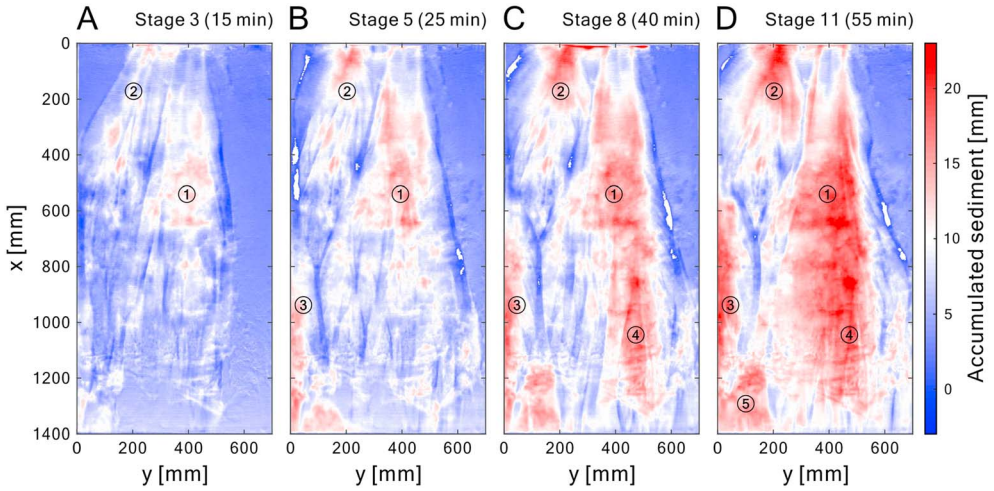

Figure 2. Accumulated sediment depositional map of Run A3 at times 15, 25, 40, and 55 min. *x* denotes downstream direction; *y* denotes cross-stream direction. Blue area represents the regions that are less affected by density currents. White areas are the region where sediment accumulated approximately to 10 mm. Red areas are the region where sediments are more than 10 mm thick.

we turned off the inflow and scanned the submarine bed surface. We used a topographic imaging system [*Huang et al.*, 2010; *Lai et al.*, 2016] to construct high-resolution digital elevation models (DEMs) of the submarine bed surface over successive stages. We further draped the calibrated color images at the end of each stage onto the DEMs to visualize submarine braided channels in detail (Figure 1).

We measured braiding intensities of the submarine channel networks by mapping from the orthorectified images, which were translated from the DEMs. For each run we selected 30 to 40 calibrated orthophotos (at 150 s intervals after t = 150 s) and measured visually the total number of channels occupied by density current at six fixed transects at 200 mm intervals from 200 to 1200 mm downstream from the inlet. We calculated the (integer) number of active and total submarine channels from these orthophotos along each transect. Active channels were identified by tracing visible bed material movement from successive orthophotos. For each orthophoto, we report the (real-valued) mean and standard deviation of active and total channels over the six profiles as a representation of the instantaneous braiding intensities.

3. Results

The general development of braided planform morphology was similar in all six experiments (Figure S2 in the supporting information). The surface evolution of the submarine channels observed in Run A3 is shown in Figure 1 as a representative example. The saline underflow evolved from an unconfined, bottom-hugging density current $<$3 mm thick, which entrained a negligible amount of ambient water, into a dynamic, multithreaded morphology (Movies S1 and S2 in the supporting information). In the early stages (Stages 1 to 3), the thin, unconfined density current spread out and bypassed the flat sedimentary basin. Sediment transported by the saline current, on the contrary, moved relatively slowly and advanced downstream via a set of switching lobes. By Stage 5 (Figure 1b), the current constructed multiple submarine channels. By Stage 8, the growth of dynamic channels and bars was significant. Some old channels and bars were eroded and cut through by newly formed channels. We observed four main active channels that rapidly transported bed load material from the sediment source to the deep sink. These active channels significantly modified the bed through channel migration and avulsion. By Stage 11, active channels shifted and replaced the inactive channels. The total number of channels increased to seven to eight on average. We subtract the DEM of the original bed surface from the reconstructed DEMs of each stage to generate cumulative depositional maps (Figure 2). As shown in Figures 2a–2c, deposition and bar growth occurred via a spatial patchwork of depositional regions that expanded (both laterally and longitudinally) and merged to create the overall braided morphology.

Instead of using fluvial-limited empirical relations for distinguishing channel patterns [*van den Berg*, 1995; *Kleinhans and van den Berg*, 2011], we find that the depth:width (aspect) ratio of the flow successfully

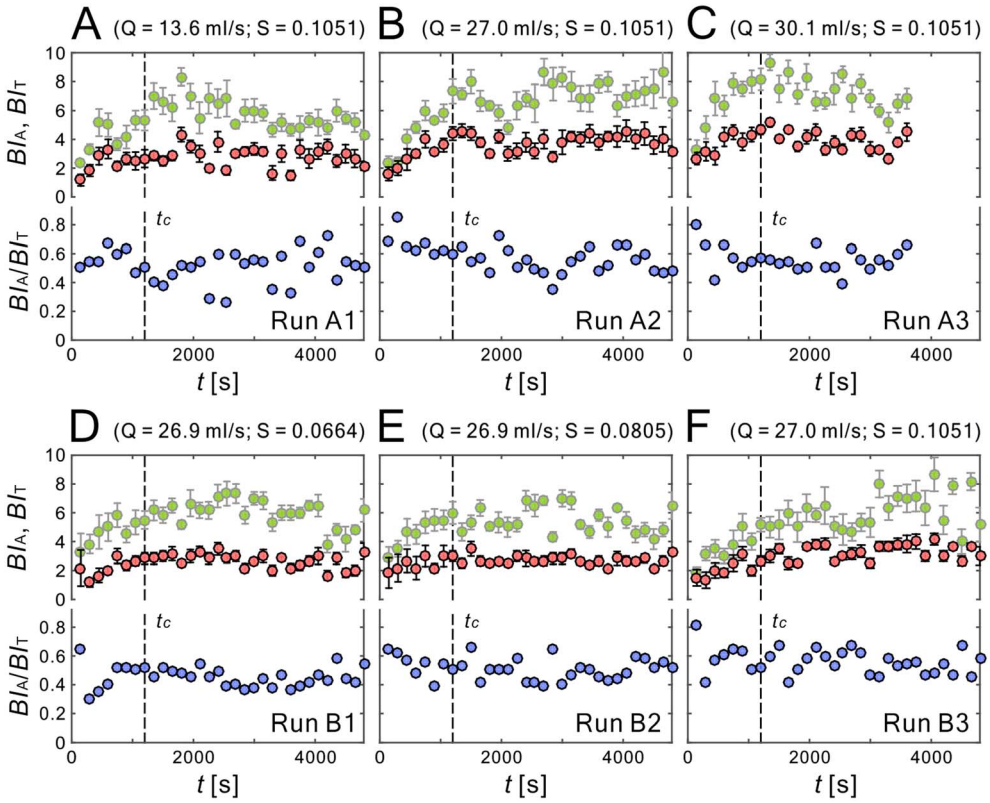

Figure 3. Total braiding intensity (BI_T, green dots), active braiding intensity (BI_A, red dots), and the ratio of BI_A to BI_T (blue dots) for experimental submarine braided channels from our six runs. The time threshold (t_c = 1200 s) separates the increasing phase and stable phase. See Table S3 in the supporting information for tabulated values.

predicts most of the planform morphology of submarine channels according to the stability theory of *Parker* [1976], confirming to the results of *Foreman et al.* [2015]. In addition to the data presented in *Parker* [1976] and *Foreman et al.* [2015], we included the braided channels of our six experiments, as well as 12 new field [*Klaucke et al.*, 1997; *Estrada et al.*, 2005; *Dowdeswell et al.*, 2008; *Gardner*, 2010] and experimental [*Keevil et al.*, 2007; *Peakall et al.*, 2007] data sets from the literature onto the theoretical prediction for channel patterns (Figure S3 and Table S2 in the supporting information). Although the stability theory of *Parker* [1976] overpredicts the braids of our experiments and incorrectly predicted some of the submarine channels, the theory successfully predicted the majority of observations and provides a robust physics-based reference for categorizing channel patterns in both fluvial and submarine environments.

We measured the instantaneous total braiding intensity (BI_T), active braiding intensity (BI_A), and the ratio of BI_A to BI_T of our six experiments. As shown in Figure 3, both BI_T and BI_A increase with higher water discharge Q, i.e., comparatively lower Qs/Q ratio (Runs A1, A2, and A3), and steeper basement slope (Runs B1, B2, and B3). In all experiments, braiding intensities gradually reach a stable phase with no further change, after a short transient phase of increase. For our six runs, the values of BI_T are all greater and show more variability than those of BI_A. We used a fixed time threshold (t_c = 1200 s) for all the runs to distinguish between the transient phase and stable phase and calculated the average values of BI_T, BI_A, and the ratio of BI_A to BI_T in the stable phase to represent braiding intensities (Tables S1 and S3 in the supporting information). Although individually BI_T and BI_A vary in time, the ratio of BI_A to BI_T for each run gradually approached a consistent value of 0.5 (±0.05).

4. Discussion

Based on our experimental results and observations, the value of BI_T, on average, is about twice BI_A over the duration of the experiment. This finding implies that as is the case in rivers, the submarine channel network is

formed progressively by migration and avulsion of active channels. Active channels become inactive, and we observed that these inactive channels serve as preferred routes for future channel bifurcations or partial avulsions. Both BI_T and BI_A are proportional to the inflow discharge and basement slope and reach equilibrium values. These trends are the same as in braided river experiments [*Bertoldi et al.*, 2009; *Egozi and Ashmore*, 2009] and indicate that the planform geometry of submarine braided channels reaches a dynamic equilibrium for a fixed discharge and bed slope. The gradual initial increase in BI_T and BI_A is also similar to fluvial experiments [*Egozi and Ashmore*, 2009]. However, a noteworthy difference with the fluvial experiments is that this initial-increase phase is shorter in our experiments (in the form of dimensionless time, $t^* = tQ/{d_s}^3$; t^* = 2.0E +10 averaged from our six runs, compared to t^* = 8.8E+10 for experiment 7 of *Egozi and Ashmore*, 2009). A possible reason is that we released an unconfined density current on a steep, initially flat sediment bed instead of confining the initial flow in a mild, prescribed straight channel, as is typically done in studies of meandering and braided rivers [*Schumm et al.*, 1987; *Bertoldi et al.*, 2009; *Egozi and Ashmore*, 2009]. Therefore, our experimental design may speed up the initial formation of multiple channels and bars and hence the approach to a dynamic steady state. Another possible reason for the faster development of braiding in our experiments is that we used plastic sediment (specific gravity = 1.5) instead of typical mineral sand (specific gravity = 2.65), thus providing higher bed mobility (see Shields numbers in Table S4 in the supporting information). The unconfined density currents can easily expand and find their routes downstream to generate at least two to three active multithread channels rather than a single, active, multithread channel. Therefore, the values of BI_A in our experiments are approximately 2 times higher than those for experimental braided rivers [*Egozi and Ashmore*, 2009]. This is consistent with the finding of *Bertoldi et al.* [2009] that higher bed mobility results in higher BI_A. Notably, the ratio of BI_A to BI_T in all six of our experiments converged around 0.5 during the stable phase. This result is close to that of *Egozi and Ashmore* [2009], who measured a constant BI_A to BI_T ratio averaging 0.4. Thus, the planimetric configuration in our submarine braided system reached a dynamic steady state with similar active fraction as fluvial braiding, but faster. This observation suggests inherent instabilities within the bifurcations of both rivers and submarine channels, or alternatively, that prior to bifurcation the channel was close to the critical shear stress for bed load transport and could not maintain transport simultaneously in both channels [*Egozi and Ashmore*, 2009]. If the latter condition holds, one would predict greater BI_A to BI_T ratios when bed mobility is greater. Our data are consistent with this relationship, but this question deserves further study, e.g., quantitative comparisons between fluvial and submarine braided channels with identical sediment properties, initial channel geometry, and flow conditions or quantitative comparisons between our system (Figure S4) to large-scale depositional system, as experimental alluvial fans [*van Dijk et al.*, 2012] or submarine fans [*Cantelli et al.*, 2011].

Bertoldi et al. [2009] and *Egozi and Ashmore* [2009] related braiding geometry to stream power for experimental fluvial channels. To relate these results to our new data for submarine channels, we propose a modified dimensionless stream power (ω^*) to include the effect of reduced gravity within the density underflow, defined as

$$\omega^* = \frac{(\rho_{\text{in}} - \rho_a)QS}{\rho_{\text{in}} w_s {d_s}^2}, \tag{1}$$

where ρ_{in} is inflow density (saline, ρ_{in} = 1200 kg m^{-3}); ρ_a is ambient density (water, ρ_a = 1000 kg m^{-3}); Q is inflow discharge; S is bed slope; d_s is median grain size diameter (d_s = 0.34 mm); and w_s is sediment settling velocity based on *Ferguson and Church* [2004]

$$w_s = \frac{R g {d_s}^2}{C_1 \nu + \left(0.75 C_2 R g {d_s}^3\right)^{0.5}}, \tag{2}$$

where $R = (\rho_s/\rho_{\text{in}} - 1)$ is submerged relative density of sediment (R = 0.25 in this study); ρ_s is sediment density (plastic sand, ρ_s = 1500 kg m^{-3}); ν is water kinematic viscosity ($\nu = 10^{-6}$ m^2 s^{-1}); and C_1 = 18 and C_2 = 1 are constants for typical natural sands [*Ferguson and Church*, 2004]. We found that similarly to rivers, the representative BI_A of our submarine braided channels scales linearly with the dimensionless stream power ω^* (Figure 4). This supports use of the reduced-gravity stream power (equation (1)) to compare density currents and fluvial processes. In our cases (Runs A1, A2, and A3), with fixed slope, increasing inflow discharge resulted in higher values of BI_A. Similarly, with fixed inflow discharge (Runs B1, B2, and B3), steeper basement slope also resulted in higher BI_A. These results agree with those for experimental rivers [*Bertoldi et al.*, 2009; *Egozi*

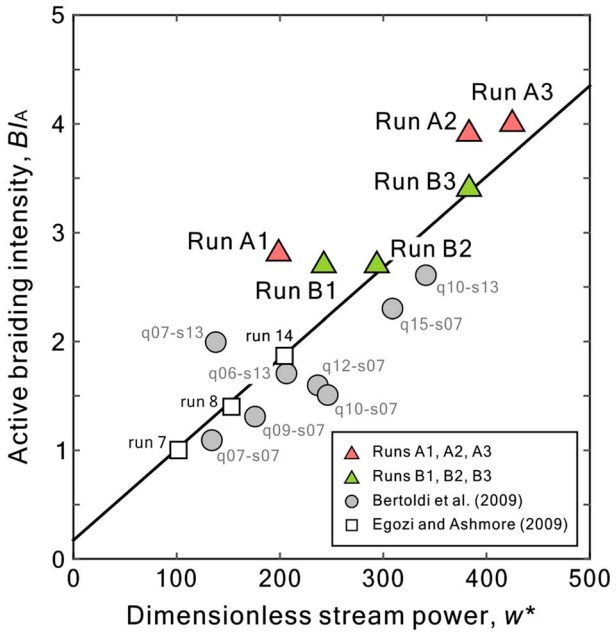

Figure 4. Active braiding intensity (BI_A) versus dimensionless stream power (ω^*) for this study, as well as data from *Bertoldi et al.* [2009] and *Egozi and Ashmore* [2009]. Solid line is a linear least squares fit ($y = 0.0084x + 0.17$ and $R^2 = 0.75$) to the fluvial and submarine data. See equation (1) for the definition of dimensionless stream power and Tables S1 and S3 in the supporting information for the tabulated values.

and Ashmore, 2009], which show that dimensionless stream power strongly influences the active braiding intensity, and with field observations for rivers [*Goff and Ashmore*, 1994].

In many ways this finding makes the rare braided turbidity and density channels identified in nature even more enigmatic. On modern Earth and in the stratigraphic record, multithread submarine channels tend to be associated with shallow slopes, reduced suspended sediment loads, and coarser sediment bed loads compared to their sinuous, single-channel counterparts [*Hein and Walker*, 1982; *Ercilla et al.*, 1998; *Hesse et al.*, 2001; *Wynn et al.*, 2007; *Piper and Normark*, 2009]. Moreover, the braided channels originate from single-thread channels found upslope, which likely results in progressively lower discharges as flow is lost to overspill processes [*Peakall et al.*, 2007]. These factors—reduced inflow density, lower discharge, shallower slope, and larger bed grain size—act to decrease the dimensionless stream power and thus should decrease the active braiding intensity. On the other hand, braiding is promoted by loss of flow confinement, which, in general, should increase width and decrease depth. We suggest that the relative rarity of braiding in submarine depositional systems indicates that it is difficult for simple spreading of the flow to produce sufficiently low depth:width ratios, given that the reduced density contrast under water means that flow depth must remain relatively high to allow sediment transport. The presence of freshwater in some (hyperpycnal) turbidity currents makes this even more difficult [*Steel et al.*, 2017].

Of course, this is not an issue if some or all of the rare modern examples of braided channels are not actually braided. True braiding occurs when flow instabilities result in spontaneous bar deposition that segments the channel into multiple, simultaneously active dynamic anabranches. Superficially similar planform morphologies can be formed, for example, by purely erosive events that scour bar-like shapes from preexisting deposits and may nucleate on top of topographic features. In these cases the flow instabilities are not dynamic, autogenic features but rather are determined by extrinsic conditions. Indeed, geophysical data suggest that some modern, putatively braided, submarine channels show seismic reflectors more consistent with erosion than deposition [*Flood et al.*, 2009]; in other cases seafloor topography, such as hydrothermal vents, are imaged beneath and appear to nucleate, the "braid bars" [*Ercilla et al.*, 1998; *Flood et al.*, 2009; *Callec et al.*, 2010]. Thus, these systems may be more analogous to anabranching river channels set in bedrock rather than to braided rivers. Finally, no one has directly observed the deposition of a braid bar in a modern turbidity-current channel. The examples of braided turbidite channels in the deep stratigraphic record [e.g., *Hein and Walker*, 1982] certainly show features consistent with fluvial braiding, but ultimately, it is not possible to know definitively how many channels were simultaneously active at the time of deposition.

So the problem remains: why are braided turbidity channels so rare, or potentially absent, in nature if they are so easily produced on experimental scales? Based on our new experiments, we propose an additional hypothesis not identified in earlier work: We hypothesize that the rarity may be due to deposition within the inactive submarine channels that, in effect, self-limits the pattern development. This phenomenon may also explain why sinuous submarine channels commonly shift from early phases of incision and lateral migration to aggradation [*Covault et al.*, 2016; *Jobe et al.*, 2016]. Our line of reasoning is as follows: Inactive threads

are zones of suspended transport during bankfull flow in fluvial systems and deposition during low-flow conditions [*Ashmore*, 1982]. Putatively, this is also the case for braided submarine channels, and we posit that the greater suspended sediment concentration in turbidity currents leads to greater deposition within the inactive threads during low-flow conditions. Greater aggradation within inactive channel threads, combined with reduced density contrast between the turbidity current and ambient fluid [*Imran et al*., 1999], enhances overspill processes and would restrict active channel thread movement. This process should also act to inhibit segmentation of the flow by bars if a greater proportion of the turbidity current were displaced above the channel margins. This hypothesis predicts a stratigraphy wherein a single coarse-grained channel fill dominates the early evolution of a submarine system, with laterally equivalent or subjacent channel fills dominated by fine-grained suspended sediment deposition. If our experimental analysis is correct, we expect a 1:1 ratio of relatively coarse and relatively fine grained channel fills in the stratigraphy corresponding to active and inactive channel threads, but it also implies that braiding would be a transient feature during the early evolution of some turbidity-current systems. Infilling of inactive channels and tendency for overspill onto the adjacent levee and overbank settings would prevent the avulsion and migration patterns necessary to maintain a braided planform. This pattern should be distinguishable from lateral movement of a single, sinuous channel that would result in a series of overlapping and subjacent channel fills with similar grain size distribution [*Covault et al*., 2016; *Jobe et al*., 2016]. Two key parameters need to be altered in future experiments to test this hypothesis: (1) suspended sediment must be included within the density current and (2) currents must be episodic, with distinct low-flow or no-flow intervals rather than the continuous bankfull flow conditions in our experiments.

In nature, measuring flow and sediment flux in a single-thread channel has proven difficult, and extending such measurements to several channel threads across tens of kilometers represents an even greater challenge. If the scale independence of braided channel planform morphology holds [*Parker*, 1976; *Sapozhnikov and Foufoula-Georgiou*, 1996; *Parker et al*., 2007; *Kleinhans and van den Berg*, 2011; *Foreman et al*., 2015], it should be possible to estimate sediment flux through these multithread systems without extensive instrumental observation. Moreover, our findings suggest that geologists should observe lithologic evidence, likely in the form of grain size variation that correlates to active bed load transport (active channel) or suspended load transport (inactive transport), among exposed channels [*Hein and Walker*, 1982; *Belderson et al*., 1984; *Hesse et al*., 2001; *Callec et al*., 2010]. Feasibly, estimates of sediment flux could be generated from this information, combined with experimental results. Finally, scale independence implies that similar relationships among braiding intensity, planform morphology, and sediment transport apply generally in multithread, depositional, and channelized systems. If the braiding behavior of flows with quite different relative densities is as general as our experiments suggest, and if scale independence holds, this opens the possibility of determining paleodischarge and morphologic activity for planetary river systems, including methane rivers on Titan [*Lunine and Lorenz*, 2009] and reconstruction of those from the rock record of Mars and elsewhere. The challenges of in situ measurements of flow conditions in submarine systems on Earth and the resultant geomorphic behaviors are magnified several folds when considering extraterrestrial problems.

In closing, we summarize our experimental findings as follows: Submarine channels on a turbidite fan exhibit active channels and nonactive channels. Only active submarine channels transport bed load sediment, similarly to fluvial rivers. Total braiding intensity (BI_T) and active braiding intensity (BI_A) of the submarine braided channels are both proportional to inflow discharge and slope at steady state. These trends are similar to the trends of fluvial braided rivers reported by *Egozi and Ashmore* [2008, 2009]. Moreover, the ratio of BI_A to BI_T reaches a stable value of 0.5, comparable to the value (0.4) for braided rivers. Although the channel geometry and flow conditions between our experiments and the experiment of fluvial rivers are not identical, the consistency of the trends of BI_A and BI_T implies that submarine braided systems, like braided rivers, reach a dynamic steady state in planform morphology that reflects the formative inflow discharge and slope, i.e., stream power. Also, active braiding intensity (BI_A) of the submarine braided channels scales linearly with dimensionless stream power. This trend is likewise similar to braided rivers. Finally, our results show that the stability analysis of river planform morphology [*Parker*, 1976] additionally applies to most submarine braided channels. However, there may exist an alternative theory for a better description of the channel patterns in both fluvial and submarine systems. Detailed analyses of channel avulsion, lateral migration, the stability of the channel planform shape, long-term depositional stratigraphy, and sediment transport mechanics are not included in this study and suggest paths for further research.

Acknowledgments
This work was supported by the Ministry of Science and Technology from Taiwan (grants MOST 105-2625-M-006-008 and MOST 106-2119-M-239-001) and National Science Foundation (NSF) via the National Center for Earth-surface Dynamics. It has also been supported by the St. Anthony Falls Laboratory industrial consortium for experimental stratigraphy. Pao-Shan Yu is gratefully acknowledged for an additional grant. The data used are listed in the references, tables, and supporting information. Finally, we thank Peter E. Ashmore and Maarten G. Kleinhans for their helpful, constructive reviews.

References

Amblas, D., T. P. Gerber, B. Mol, R. Urgeles, D. Garcia-Castellanos, M. Canals, L. F. Pratson, N. Robb, and J. Canning (2012), Survival of a submarine canyon during long-term outbuilding of a continental margin, *Geology*, *40*(6), 543–546.

Ashmore, P. E. (1982), Laboratory modelling of gravel braided stream morphology, *Earth Surf. Processes Landforms*, *7*(3), 201–225.

Ashmore, P. E. (1991), How do gravel-bed rivers braid, *Can. J. Earth Sci.*, *28*(3), 326–341.

Babonneau, N., B. Savoye, M. Cremer, and M. Bez (2010), Sedimentary architecture in meanders of a submarine channel: Detailed study of the present Congo turbidite channel (Zaiango Project), *J. Sediment. Res.*, *80*(9–10), 852–866.

Belderson, R., N. Kenyon, A. Stride, and C. Pelton (1984), A "braided" distributary system on the Orinoco deep-sea fan, *Mar. Geol.*, *56*(1), 195–206.

Bertoldi, W., L. Zanoni, and M. Tubino (2009), Planform dynamics of braided streams, *Earth Surf. Processes Landforms*, *34*(4), 547–557.

Callec, Y., E. Deville, G. Desaubliaux, R. Griboulard, P. Huyghe, A. Mascle, G. Mascle, M. Noble, C. P. de Carillo, and J. Schmitz (2010), The Orinoco turbidite system: Tectonic controls on sea-floor morphology and sedimentation, *AAPG Bull.*, *94*(6), 869–887.

Cantelli, A., C. Pirmez, S. Johnson, and G. Parker (2011), Morphodynamic and stratigraphic evolution of self-channelized subaqueous fans emplaced by turbidity currents, *J. Sediment. Res.*, *81*(3–4), 233–247.

Covault, J. A., Z. Sylvester, S. M. Hubbard, Z. R. Jobe, and R. P. Sech (2016), The stratigraphic record of submarine-channel evolution, *The Sediment. Rec.*, *14*(3), 4–11.

Deptuck, M. E., Z. Sylvester, C. Pirmez, and C. O'Byrne (2007), Migration-aggradation history and 3-D seismic geomorphology of submarine channels in the Pleistocene Benin-major Canyon, western Niger Delta slope, *Mar. Pet. Geol.*, *24*(6–9), 406–433.

Dowdeswell, J., C. Ó. Cofaigh, R. Noormets, R. D. Larter, C.-D. Hillenbrand, S. Benetti, J. Evans, and C. Pudsey (2008), A major trough-mouth fan on the continental margin of the Bellingshausen Sea, West Antarctica: The Belgica Fan, *Mar. Geol.*, *252*(3), 129–140.

Egozi, R., and P. Ashmore (2008), Defining and measuring braiding intensity, *Earth Surf. Processes Landforms*, *33*(14), 2121–2138.

Egozi, R., and P. Ashmore (2009), Experimental analysis of braided channel pattern response to increased discharge, *J. Geophys. Res.*, *114*, F02012, doi:10.1029/2008JF001099.

Ercilla, G., B. Alonso, J. Baraza, D. Casas, F. Chiocci, F. Estrada, M. Farran, E. Gonthier, F. Perez-Belzuz, and C. Pirmez (1998), New high-resolution acoustic data from the braided system of the Orinoco deep-sea fan, *Mar. Geol.*, *146*(1), 243–250.

Estrada, F., G. Ercilla, and B. Alonso (2005), Quantitative study of a Magdalena submarine channel (Caribbean Sea): Implications for sedimentary dynamics, *Mar. Pet. Geol.*, *22*(5), 623–635.

Ferguson, R., and M. Church (2004), A simple universal equation for grain settling velocity, *J. Sediment. Res.*, *74*(6), 933–937.

Flood, R. D., R. N. Hiscott, and A. E. Aksu (2009), Morphology and evolution of an anastomosed channel network where saline underflow enters the Black Sea, *Sedimentology*, *56*(3), 807–839.

Foreman, B. Z., S. Y. J. Lai, Y. Komatsu, and C. Paola (2015), Braiding of submarine channels controlled by aspect ratio similar to rivers, *Nat. Geosci.*, *8*(9), doi:10.1038/NGEO2505.

Gardner, J. V. (2010), The West Mariana Ridge, western Pacific Ocean: Geomorphology and processes from new multibeam data, *Geol. Soc. Am. Bull.*, *122*(9–10), 1378–1388.

Goff, J. R., and P. Ashmore (1994), Gravel transport and morphological change in braided Sunwapta River, Alberta, Canada, *Earth Surf. Processes Landforms*, *19*(3), 195–212.

Hein, F. J., and R. G. Walker (1982), The Cambro-Ordovician Cap Enragé Formation, Queébec, Canada: Conglomeratic deposits of a braided submarine channel with terraces, *Sedimentology*, *29*(3), 309–352.

Hesse, R., I. Klaucke, S. Khodabakhsh, D. J. Piper, W. B. Ryan, and N. S. Group (2001), Sandy submarine braid plains: Potential deep-water reservoirs, *AAPG Bull.*, *85*(8), 1499–1521.

Huang, M. Y. F., A. Y. L. Huang, and H. Capart (2010), Joint mapping of bed elevation and flow depth in microscale morphodynamics experiments, *Exp. Fluids*, *49*(5), 1121–1134.

Imran, J., G. Parker, and C. Pirmez (1999), A nonlinear model of flow in meandering submarine and subaerial channels, *J. Fluid Mech.*, *400*, 295–466.

Jobe, Z. R., N. C. Howes, and N. C. Auchter (2016), Comparing submarine and fluvial channel kinematics: Implications for stratigraphic architecture, *Geology*, *44*(11), 931–934.

Keevil, G. M., J. Peakall, and J. L. Best (2007), The influence of scale, slope and channel geometry on the flow dynamics of submarine channels, *Mar. Pet. Geol.*, *24*(6–9), 487–503.

Kertznus, V., and B. Kneller (2009), Clinoform quantification for assessing the effects of external forcing on continental margin development, *Basin Res.*, *21*(5), 738–758.

Klaucke, I., R. Hesse, and W. Ryan (1997), Flow parameters of turbidity currents in a low-sinuosity giant deep-sea channel, *Sedimentology*, *44*(6), 1093–1102.

Kleinhans, M. G., and J. H. van den Berg (2011), River channel and bar patterns explained and predicted by an empirical and a physics-based method, *Earth Surf. Processes and Landforms*, *36*(6), 721–738.

Kleinhans, M. G., W. M. van Dijk, W. I. van de Lageweg, D. C. Hoyal, H. Markies, M. van Maarseveen, C. Roosendaal, W. van Weesep, D. van Breemen, and R. Hoendervoogt (2014), Quantifiable effectiveness of experimental scaling of river- and delta morphodynamics and stratigraphy, *Earth Sci. Rev.*, *133*, 43–61.

Kolla, V., A. Bandyopadhyay, P. Gupta, B. Mukherjee, and D. Ramana (2012), Morphology and internal structure of a recent upper Bengal fan-valley complex, in *Application of the Principles of Seismic Geomorphology to Continental-Slope and Base-of-Slope Systems: Case Studies From Seafloor and Near-Seafloor Analogues*, vol. 99, pp. 347–369, SEPM, Special Publication, Tulsa, Okla.

Lai, S. Y. J., and H. Capart (2007), Two-diffusion description of hyperpycnal deltas, *J. Geophys. Res.*, *112*, F03005, doi:10.1029/2006JF000617.

Lai, S. Y. J., and H. Capart (2009), Reservoir infill by hyperpycnal deltas over bedrock, *Geophys. Res. Lett.*, *36*, L08402, doi:10.1029/2008GL037139.

Lai, S. Y. J., T. P. Gerber, and D. Amblas (2016), An experimental approach to submarine canyon evolution, *Geophys. Res. Lett.*, *43*, 2741–2747, doi:10.1002/2015GL067376.

Lajeunesse, E., L. Malverti, P. Lancien, L. Armstrong, F. Metivier, S. Coleman, C. E. Smith, T. Davies, A. Cantelli, and G. Parker (2010), Fluvial and submarine morphodynamics of laminar and near-laminar flows: A synthesis, *Sedimentology*, *57*(1), 1–26.

Lunine, J. I., and R. D. Lorenz (2009), Rivers, lakes, dunes, and rain: Crustal processes in Titan's methane cycle, *Annu. Rev. Earth Planet. Sci.*, *37*, 299–320.

Malverti, L., E. Lajeunesse, and F. Metivier (2008), Small is beautiful: Upscaling from microscale laminar to natural turbulent rivers, *J. Geophys. Res.*, *113*, F04004, doi:10.1029/2007jf000974.

Métivier, F., E. Lajeunesse, and M.-C. Cacas (2005), Submarine canyons in the bathtub, *J. Sediment. Res.*, *75*(1), 6–11.
Paola, C., K. Straub, D. Mohrig, and L. Reinhardt (2009), The "unreasonable effectiveness" of stratigraphic and geomorphic experiments, *Earth Sci. Rev.*, *97*(1–4), 1–43.
Parker, G. (1976), On the cause and characteristic scales of meandering and braiding in rivers, *J. Fluid Mech.*, *76*(03), 457–480.
Parker, G., P. R. Wilcock, C. Paola, W. E. Dietrich, and J. Pitlick (2007), Physical basis for quasi-universal relations describing bankfull hydraulic geometry of single-thread gravel bed rivers, *J. Geophys. Res.*, *112*, F04005, doi:10.1029/2006JF000549.
Parsons, D. R., J. Peakall, A. E. Aksu, R. D. Flood, R. N. Hiscott, Ş. Beşiktepe, and D. Mouland (2010), Gravity-driven flow in a submarine channel bend: Direct field evidence of helical flow reversal, *Geology*, *38*(12), 1063–1066.
Piper, D. J., and W. R. Normark (2009), Processes that initiate turbidity currents and their influence on turbidites: A marine geology perspective, *J. Sediment. Res.*, *79*(6), 347–362.
Peakall, J., B. McCaffrey, and B. Kneller (2000), A process model for the evolution, morphology, and architecture of sinuous submarine channels, *J. Sediment. Res.*, *70*(3), 434–448.
Peakall, J., K. J. Amos, G. M. Keevil, P. W. Bradbury, and S. Gupta (2007), Flow processes and sedimentation in submarine channel bends, *Mar. Pet. Geol.*, *24*(6–9), 470–486.
Peakall, J., I. A. Kane, D. G. Masson, G. Keevil, W. McCaffrey, and R. Corney (2012), Global (latitudinal) variation in submarine channel sinuosity, *Geology*, *40*(1), 11–14.
Rowland, J. C., G. E. Hilley, and A. Fildani (2010), A test of initiation of submarine leveed channels by deposition alone, *J. Sediment. Res.*, *80*(8), 710–727.
Sapozhnikov, V., and E. Foufoula-Georgiou (1996), Self-affinity in braided rivers, *Water Resour. Res.*, *32*(5), 1429–1439, doi:10.1029/96WR00490.
Schumm, S. A., M. P. Mosley, and W. E. Weaver (1987), *Experimental Fluvial Geomorphology*, 413 pp., Wiley, New York.
Steel, E. S., J. Buttles, A. R. Simms, D. Mohrig, and E. Meiburg (2017), The role of buoyancy reversal in turbidite deposition and submarine fan geometry, *Geology*, *45*(1), 35–38.
Straub, K. M., D. Mohrig, B. McElroy, J. Buttles, and C. Pirmez (2008), Interactions between turbidity currents and topography in aggrading sinuous submarine channels: A laboratory study, *Geol. Soc. Am. Bull.*, *120*(3–4), 368–385.
Sumner, E. J., J. Peakall, R. M. Dorrell, D. R. Parsons, S. E. Darby, R. B. Wynn, S. D. McPhail, J. Perrett, A. Webb, and D. White (2014), Driven around the bend: Spatial evolution and controls on the orientation of helical bend flow in a natural submarine gravity current, *J. Geophys. Res. Oceans*, *119*, 898–913, doi:10.1002/2013JC009008.
Tal, M., and C. Paola (2007), Dynamic single-thread channels maintained by the interaction of flow and vegetation, *Geology*, *35*(4), 347.
van den Berg, J. H. (1995), Prediction of alluvial channel pattern of perennial rivers, *Geomorphology*, *12*(4), 259–279.
van Dijk, M., M. G. Kleinhans, G. Postma, and E. Kraal (2012), Contrasting morphodynamics in alluvial fans and fan deltas: Effect of the downstream boundary, *Sedimentology*, *59*(7), 2125–2145.
Weill, P., E. Lajeunesse, O. Devauchelle, F. Metiver, A. Limare, B. Chauveau, and D. Mouaze (2014), Experimental investigation on self-channelized erosive gravity currents, *J. Sediment. Res.*, *84*(6), 487–498.
Wynn, R. B., B. T. Cronin, and J. Peakall (2007), Sinuous deep-water channels: Genesis, geometry and architecture, *Mar. Pet. Geol.*, *24*(6–9), 341–387.
Wynn, R. B., et al. (2014), Autonomous Underwater Vehicles (AUVs): Their past, present and future contributions to the advancement of marine geoscience, *Mar. Geol.*, *352*, 451–468.
Yu, B., A. Cantelli, J. Marr, C. Pirmez, C. O'Byrne, and G. Parker (2006), Experiments on self-channelized subaqueous fans emplaced by turbidity currents and dilute mudflows, *J. Sediment. Res.*, *76*(6), 889–902.